HYDRIC EROSION MAPPING ENHANCEMENT IN KORIFLA SUB-WATERSHED (CENTRAL MOROCCO)

FATIMAZAHRA EDDEFLI[1], MOHAMED TAYEBI[1], SOUFIANE HAJAJ[2*], ACHRAF KHADDARI[1], ABDELHADI OUAKIL[3] AND ABDERRAZAK EL HARTI[2]

[1] Laboratory of Geosciences, Department of Geology, Faculty of Sciences, University Ibn Tofail, Kénitra, BP 133, Morocco
[2]Team of Remote Sensing and GIS Applied to Geosciences and Environment, Faculty of Sciences and Techniques, PO BOX. 52. Phone number: +212681100407
[3] Laboratory of Natural Resources and Sustainable Development, Department of Geology, Faculty of Sciences, University Ibn Tofail, Kénitra, BP 133, Morocco
**Corresponding author email: soufianehajaj13@gmail.com.*

Received: 15th July 2023, **Accepted:** 15th November 2023

ABSTRACT

In recent years quantitative and qualitative methods integration has become common in investigating and modeling hydric erosion. The present study focuses on using a synergistic approach of the Erosion Potential Model (EPM) and Priority Actions Program/Regional Activity Centre (PAP/RAC) in order to model the potential erosion in the Korifla Sub-watershed, Central Morocco. The combination of remotely sensed data and the EPM parameters demonstrated that the amount of soil estimated loss in the study area is between 0.001 $m^3/km^2/y$ and 68.26 $m^3/km^2/y$. Furthermore, AUC (Area Under Curve) was computed to validate the EPM modeling results by implementing 162 high erosion sites, the AUC value indicates good mapping results (0.76). The PAP/RAC model shows that in the entire study area, the zones of very high and high erosion represent respectively 10.31 % and 14.53 %, whereas the equivalent of these zones by EPM represents 6.31 % and 9.52 %. The distribution of high-erosion areas correlates well with that of moderate to steep slopes, principally in forest and agricultural lands within the study area. However, the employed methods in this study successfully simulated erosion quantitatively as well as qualitatively. The findings of this study imply that hydric erosion can threaten ecological sustainability and agricultural production in several parts of the Korifla sub-watershed. Consequently, the present study results offer valuable insights for planning efficient erosion control strategies as well as redirecting soil and slope management. To sum up, the findings of this research have important implications for implementing efficient erosion control measures in north-western central Morocco, semi-arid area.

Keywords: Hydric Erosion, GIS, EPM, PAP/RAC, Semi-arid region.

INTRODUCTION

The process of soil formation spans thousands of years, yet its degradation can occur within a relatively short timeframe. Soil erosion is widely recognized in the Mediterranean region as the predominant form of environmental degradation, exerting significant impacts on environmental and socio-economic features (PAP/CAR, 1998). Approximately 85 % of

global land degradation stems from soil loss, leading to a 17 % decline in yields (Siddique *et al*., 2017). Globally, this environmental risk poses threats to human activities, agriculture, and infrastructure, influencing the lifespan, size, and preservation of dam reservoirs. Many research has been done in Morocco on hydric erosion using PAP/RAC qualitative model, that demonstrates great modeling efficiency e. g., (Diani *et al.*, 2023; HILI *et al.*, 2017; Mesrar *et al*., 2015; Rhouma *et al*., 2018). In recent years, the integration of quantitative and qualitative methods has become common in investigating and modeling some environmental threats, such as water erosion (Elbadaoui *et al*., 2023), and landslide risk (Biswakarma *et al*., 2023). It is important to note that synergistic application of quantitative and qualitative approaches can improve several environmental risks assessment, following robust analysis of remote sensing (RS) datasets.

The EPM model (Erosion Potential Method) was developed by Gavrilovic in 1988 and has been used in several studies (Ahmed *et al.*, 2019; Amini *et al*., 2014; Efthimiou & Lykoudi, 2016; Kouhpeima *et al*., 2011; Othman *et al*., 2023; Pavlova-Traykova, 2022; Zahnoun *et al*., 2019). This method is based on three essential factors: the temperature coefficient (T), the mean annual precipitation (H), and the potential erosion parameter (Z). On the other hand, qualitative methods allow us to visualize the most vulnerable areas and their spatial distribution. (The Priority Actions Program/Regional Activity Center) (PAP/ RAC). It is a method for modeling erosive conditions, assessing the spatial distribution of risks, mapping and identifying the most vulnerable areas (Chikh *et al*., 2019; Diani *et al*., 2023; Elbadaoui *et al*., 2023). It is based on guidelines that follow three hierarchical phases namely, (i) The predictive approach, which involves applying matrices to intersect the erodibility map and the soil protection map; (ii) The descriptive approach, which focuses on the erosion pattern map; (iii) The integration approach, which implements the PAP/RAC map. However, EPM and PAP/CAR models make mutual use of GIS and remote sensing to assess erosion processes and produce land use maps (De Roo, 1998).

In Morocco, water erosion in watersheds imposes significant costs on the Moroccan economy in terms of reduced land productivity and adverse downstream consequences. The latter can be seen in the silting-up of dams and hill lakes (El Garouani *et al.*, 2003). The total lost capacity is around 1100 mm^3, nearly 6 % of the dam storage capacity (Badraoui & Hajji, 2001). When designing projects related to renewable natural resources, it is crucial to consider the significant influence of sediment production and surface erosion (Tangestani, 2006). In this context, hydric erosion is a natural risk that must be carefully studied to prevent and minimize its impact on a specific area. The study of vulnerable areas to erosion is an environmental priority. Several quantitative methods can be used to estimate hydric erosion, including empirical models including USLE (Alewell *et al*., 2019), RUSLE (El Jazouli *et al*., 2019; Hagras, 2023), EPM (Baharvand & Pradhan, 2022; Mosaid *et al*., 2022), SWAT (Alitane *et al*., 2022).). Moreover, modified methods can be applied as well as integrated methods with other data types including, magnetic susceptibility techniques (MS) combined with GIS (Mosaid *et al*., 2022). Despite the fact that some studies on hydric erosion have been conducted in the Bouregreg watershed (Eddefli *et al*., 2023; Moudden *et al*., 2022). There is a limited amount of in-depth research conducted on the Korifla sub-watershed hydric erosion. This study advances our understanding of the causality of soil erosion on a small scale in the Korifla sub-watershed. The resulting sedimentation undoubtedly impacts the storage capacity of the Sidi Mohammed Ben Abdelah dam, thereby threatening its sustainability. Therefore, it is asserted that effective conservation planning and sustainable land management practices at the watershed level are crucial for maintaining significant downstream projects. Accordingly, the current study aims to use PAP/RAC and EPM models in enhancing the hydric erosion mapping within Korifla sub-watershed (Bouregreg

watershed, Central Morocco). Following a synergistic approach using EPM with the PAP/RAC model, we provide a comprehensive perspective on the erosion state. The results obtained from this dual approach offer a thorough evaluation that encompasses both qualitative and quantitative aspects. These findings serve as a robust foundation for making well-informed decisions and ensuring sustainability.

MATERIAL AND METHODS

Study area characteristics

The Korifla sub-watershed area belongs to the Bouregreg watershed, located in the central region of Morocco, between latitudes 33°0'0" N and 33°55'0" N and longitudes 6°25'0" W et 6°55'0" W. The study area encompasses several communes, namely Brachoua, Merchouche, Rommani, Lagnadiz, Oulad ftata and Oulad boughadi (Fig.1).

Fig. 1: Geographic location map of the Korifla sub-watershed area

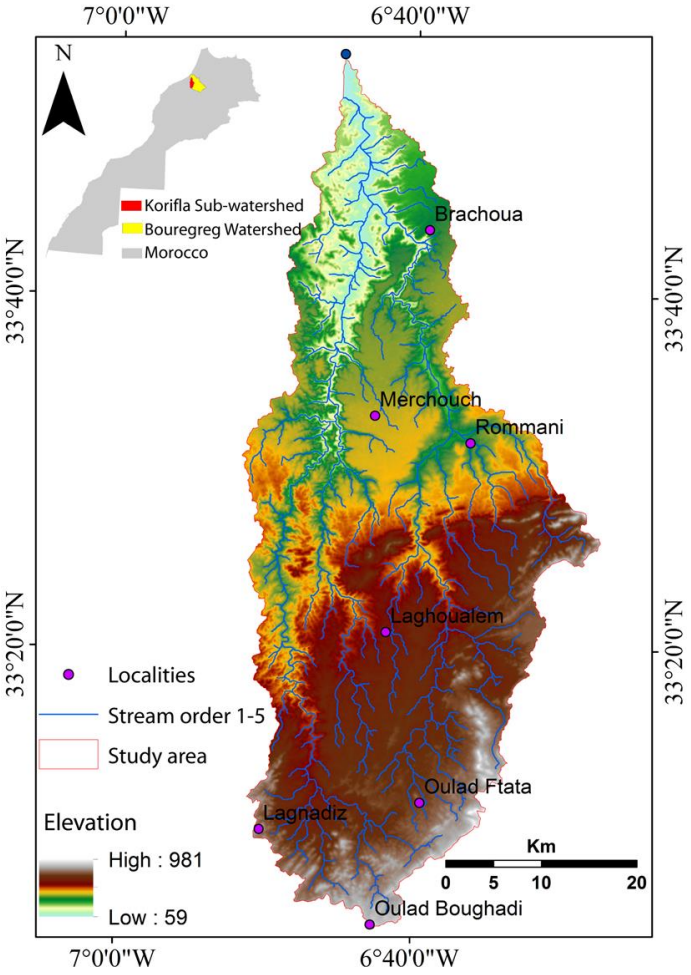

This watershed has a rugged topography. The region's climate is typically semi-arid, with average annual temperatures ranging between 18 °C and 32 °C. The average annual precipitation in this area is of medium intensity, varying between 31 mm and 35 mm. The measured average precipitation represents a major challenge for water management in the region. The study area belongs to the Moroccan Central Plateau. The dominant geological formations are of sedimentary origin, dating from the Paleozoic era. It includes several granitic batholiths and large outcrops of metamorphic rocks. The study area was folded and traversed by intrusive rocks and metamorphosed during the Hercynian orogeny, eroded during the Permian and Triassic periods. The study area is partially covered by Triassic salt-bearing red clays Secondary deposits and highly altered basalts (Beaudet, 1969) (Fig.2).

Fig. 2: Geological map of the study area within Bouregreg watershed (Laouina & Mahé, 2013)

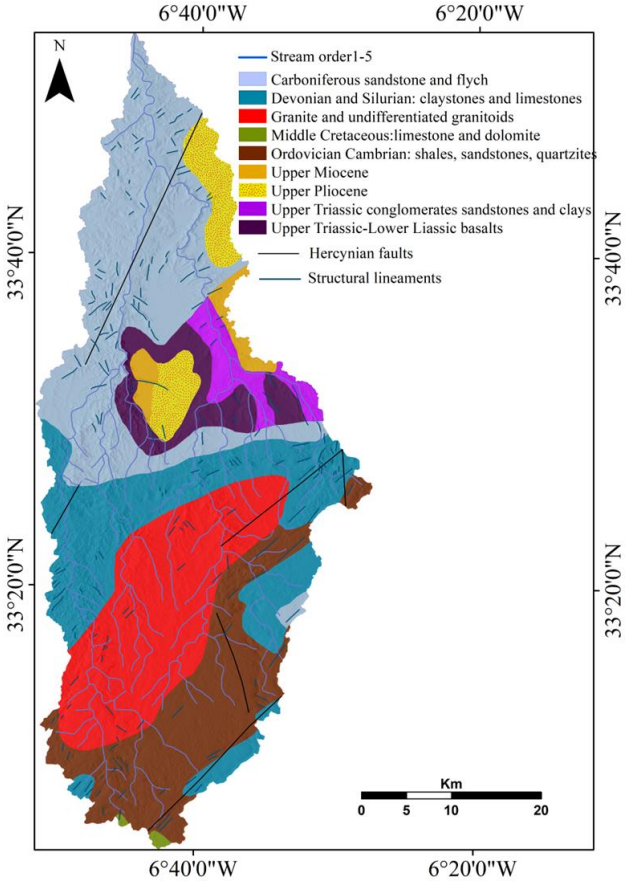

Hydric erosion dataset

This investigation methodology is based on two different models, first, the EPM model and second PAP/RAC models applied based on thematic maps, remote sensing data and field data (Table 1). They are collected from different sources, integrated, corrected, processed, and analyzed principally in GIS environment, in the order to establish a hierarchical relationship between the parameters and causative factors of erosion.

Table 1: Data sources (Abbreviation: ABHBC: Bouregeg and Chaouia Hydraulic Bassin Agency, DEM: digital elevation model, NDVI: Normalized Difference Vegetation Index)

Data	Source	Descriptions
Rainfall data	ABHBC	Spreadsheet file
Soil type Lithology	Soil map of central Morocco Bouregreg Geological map	Scale 1/50000
Temperature	www.earthexplorer.com	Landsat 8 OLI image - Band 10
DEM NDVI	www.earthexplorer.com	ASTER DEM (30 m) Landsat 8 OLI

Models

Erosion Potential Method (EPM)

Erosion Potential Method is widely recognized for its significant dependability in accurately determining sediment yields, sedimentation in reservoirs, and transport (Ristić *et al*., 2011). It can be played in the identification of erosion and degradation sensitive zones, which includes analyzing the natural factors and anthropogenic activities effects (Gocić *et al.*, 2020). The EPM Model equation is as follows (1) (Gavrilovic, 1988):

$$W=T.H.\boldsymbol{\pi}.\sqrt{Z^3} \qquad (1)$$

Where:
W: Average annual soil erosion ($m^3/km^2/y$)
T: Temperature coefficient
H: Mean annual precipitation (mm /y)
$\boldsymbol{\pi}$: 3.1415
Z: Erosion coefficient

We can use equation (2) for mean annual temperature (T) calculation (Gavrilovic, 1988):

$$T=\sqrt{(\frac{\theta}{10}+0.1)} \qquad (2)$$

Where, θ is the Annual temperature (°C)

Water erosion is mainly controlled by climate, temperature and solar radiation, which are the parameters that influence soil conditions on a large scale (Mosaid *et al*., 2022). For temperature, it is as a parameter influencing erosion within the EPM model, recognizing the capacity of thermal fluctuations to facilitate the gradual dismantling of geological elements and lithological formations. (Marouane *et al*., 2021). The mean annual temperature (T) is

obtained from the surface temperature of clear, cloud-free satellite images, where Landsat 8 operational land imager (OLI) thermal band 10 was used. This procedure is applied to all images bands for each month over the period 1997 to 2020. The annual mean temperature was obtained by applying equation (2) (Fig. 3a). Additionally, the precipitation data as well plays a direct role in triggering runoff and material transport (Nunes *et al*., 2011). Average annual rainfall (H) is derived from rainfall data for the period between 1997 and 2020 by interpolating points from stations covering the watershed (Fig. 3b). The erosion coefficient (Z) is expressed (Staut, 2004) by the equation (3):

$$Z = Xa * Y * \phi * \sqrt{Ja} \qquad (3)$$

Where the land use coefficient index (Xa) is calculated using equation (4) which depends on NDVI (Normalized Difference Vegetation Index) so the value becomes between the lowest value 0.01 and the highest 1 (Fig. 3c):

$$Xa = (XaNDVI - 0.61) * (-1.25) \qquad (4)$$

Where:

XaNDVI: Vegetation cover coefficient modified to adapt to soil protection index criteria. NDVI (eq 5) (Tucker, 1979):

$$NDVI = \left(\frac{NIR - RED}{NIR + RED}\right) \qquad (5)$$

The coefficient of soil resistance to erosion (Y) is implemented, as erosion directly affects the soil, and can be extracted from the soil map. In this study, the coefficient of soil resistance to erosion is equivalent to the K factor of the RUSLE model carried out on the same study area (Eddefli *et al*., 2023). Thus, the coefficient for observed erosion processes (Φ) is extracted from satellite images using band 4 of the Landsat 8 OLI image (Zorn & Komac, 2009), it is calculated by equation (6):

$$\Phi = \sqrt{\left(\frac{OLI4}{Qmax}\right)} \qquad (6)$$

Where Qmax: maximum radiance value

Parameter (Ja) expresses the slope, where, GIS environment can be used to calculate the slope as a percentage using digital elevation model (DEM). To apply equation (3), the coefficient (Xa) corresponding to soil cover and soil sensitivity to erosion (Φ), as well as the slope coefficient (Ja) and soil sensitivity to erosion (Y) were considered. The integration of these four parameters enables us to model the potential erosion parameter (Z).

Fig. 3: Maps used to estimate erosion: (a) Temperature, (b) Rainfall, (c) NDVI, (d) slope, (e) vegetation density, (f) land use/ land cover

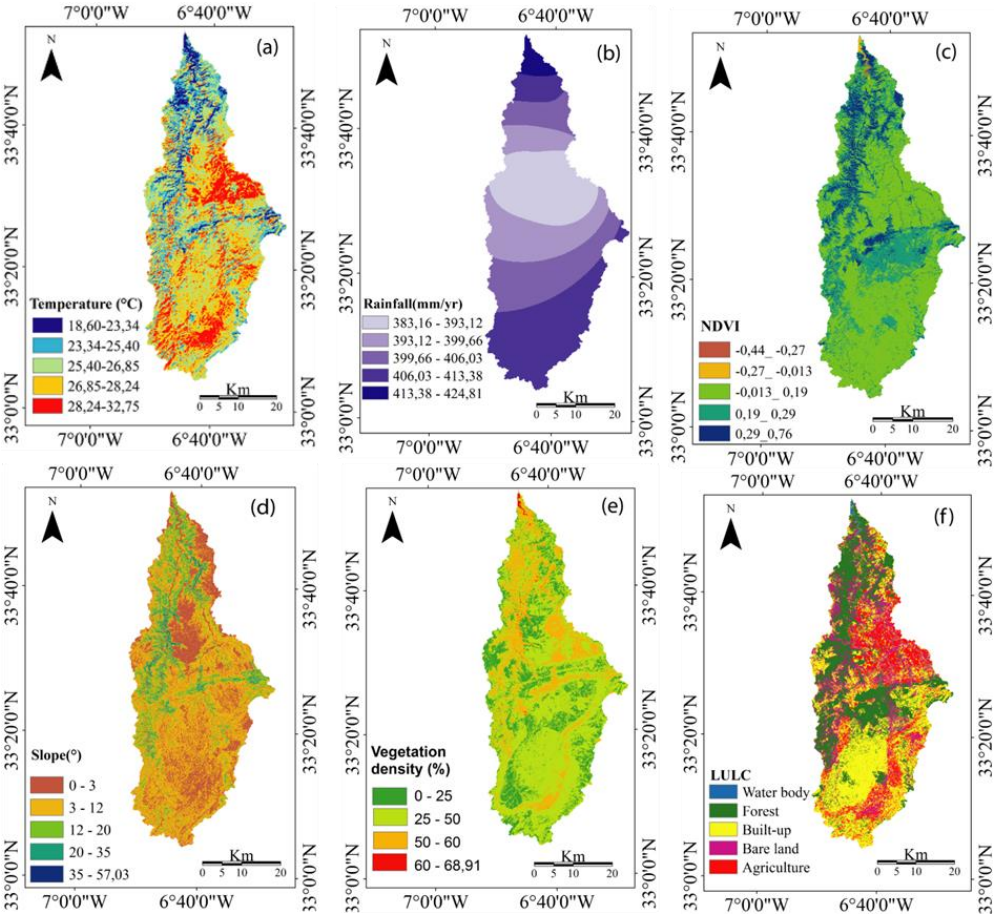

Priority Actions Programme Regional Activity Centre (PAP/RAC) model

In 1990, the FAO (Food Ans Agriculture Organization), DGCONA (Directorate-General for Nature Conservation Madrid) and PAP/PAM (Priority Action Plan for the Mediterranean) collaborated to set up a standardized methodology for mapping the state of erosive risk (Rhouma *et al*., 2018). The predictive approach aims to produce two thematic maps:

- The erodibility map resulting from the intersection of the slope map (Fig. 3d) and the lithology map.
- Soil protection map, produced by intersecting the vegetation cover map (Fig. 3e) and the land use map (Fig. 3f).

Each map was subjected to the application of the appropriate PAP/RAC-defined matrices as demonstrated in method guidelines (see Table 2). The slope map in degree was obtained from the DEM (30m), then reclassified according to (Table 3) of PAP/RAC classification following codes ranging from 1 to 5 (from the least steep slope to the maximum value which means extremely steep slope).

Table 2: Correlation matrix between land use/ land cover and vegetation density according to PAP /RAC guidelines

		Vegetation density			Land Use/ Land Cover		
PAP / RAC	**Degrees**	**Classes**	**Area(Km²)**	**percentage**	**Classes**	**Area(Km²)**	**percentage**
1	Very low	<25%	8,52	0,46	Bare land	340,14	18,51
2	Low	25- 50%	356,69	19,41	Agricultural area	256,93	13,98
3	Medium	50-75%	1472,32	80,13	Built-up	680,04	37,01
4	High	>75%	-	-	Forest area	556,16	30,27
5	Very high	-	-	-	Water body	4,28	0,23

		Vegetation density			
		1	2	3	4
LULC	1	5	5	4	4
	2	5	5	4	3
	3	3	2	1	1
	4	4	3	2	1
	5	5	4	3	2

For soil type, values tending towards one indicate low sensitivity to erosion, and values close to five indicate the high sensitivity to erosion. The same map is used for the EPM (Y) coefficient.

Reclassifying slope and lithology as well as combining these two maps is an essential step before applying the intersection matrix. The output of this process presents the erodibility map of the study area. It shows the degree of erodibility as low, moderate, medium, high or extreme. The soil protection map is the coupling between the degree of vegetation and land use by applying the matrices outlined by the PAP/RAC guidelines (Table 4). The degree of vegetation (VD) is based on two input parameters, namely (i) Advanced Vegetation Index (AVI) which is an indicator of vegetation quality and health through the red and near-infrared spectral bands corresponding to band 4 and band 5 for the Landsat 8 OLI image, (ii) Bare Soil Index (BSI) which combines the red, blue, near-infrared and Short Wave Infrared (SWIR).

Integration of both AVI and BSI data in the geographic information system produces the vegetation cover map (Fig. 2e), which shows that vegetation cover does not exceed 68.91 %. On the other hand, the Landsat 8 image is used to produce the land cover map. The image is chosen for its specific characteristics (high radiometry, cloud-free and covers the entire area). It is then subjected to supervised classification (Maximum likelihood) to map the classes' types in the study area. Thereafter, the intersection of soil protection and erodibility maps, applying the PAP/RAC matrix guideline permitted the extraction of the erosive state map of study area with five descriptive classes.

Table 3: Correlation matrix between Slope and resistance to erosion according to PAP/RAC guidelines

		Slope (°)			Resistance to erosion		
PAP/RAC	**Degree**	**Class**	**Area (Km²)**	**percentage**	**Class**	**Area (Km²)**	**percentage**
1	Very low	0-3	264,17	14,37	No resistance	131,58	7,16
2	Low	3-12	836,19	45,49	Coarse sediments	191,30	10,41
3	Medium	12-20	347,86	18,93	Low resistance	384,12	20,90
4	High	20-35	269,94	14,69	Medium resistance	256,25	13,94
5	Very high	>35	119,86	6,52	Highly resistance	874,54	47,59

		Slope (°)				
		1	2	3	4	5
Resistance to erosion	1	1	1	1	1	2
	2	1	1	2	3	3
	3	2	2	3	4	4
	4	3	3	4	5	5
	5	4	4	5	5	5

Table 4: Correlation matrix between Erodibility and soil protection according to PAP/RAC guidelines

		Erodibility			Soil protection	
PAP /RAC	**Class**	**Area (Km²)**	**percentage**	**Classes**	**Area (Km²)**	**percentage**
1	Very low	333,91	18,16	Very high	650,88	35,41
2	Low	446,26	24,28	High	359,25	19,55
3	Medium	519,19	28,24	Medium	221,93	12,07
4	High	239,65	13,04	Low	502,27	27,33
5	Very high	299,27	16,28	Very low	103,65	5,64

		Erodibility				
		1	2	3	4	5
Soil protection	1	1	1	1	2	2
	2	1	1	2	3	4
	3	1	2	3	4	4
	4	2	3	3	5	5
	5	2	3	4	5	5

RESULTS AND DISCUSSIONS

EPM

The processing results of Landsat 8 OLI thermal data show that the annual temperature is between 18.60 °C and 32.81 °C. In addition, applying equation (2) gives the temperature coefficient (T), ranging from 1.4 and 1.8. These values are proportional to relief and vegetation that can be explained by the minimum temperature values that correspond to dense vegetation and high altitudes zones; the average annual precipitation (H) ranging between 383.16 mm/y and 424.81 mm/y; the minimum values which are concentrated in the central part of the study area, where altitudes are low, compared with the southern part, where maximum precipitation values are recorded at high altitudes. Moreover, precipitation is also notable towards the outlet, as it approaches the Atlantic Ocean.

The results of equation (4) show that the soil cover coefficient (Xa) (Fig. 4a) is between 0.01 and 1, with 40.35 % of the area having a moderate coefficient and 44.17 % having a low Xa value. The high value covers a small area, with 0.01 corresponding to low vegetation cover and 1 to dense vegetation. Most areas, therefore, have medium to low vegetation cover.

Table 5 shows that soil sensitivity to erosion (Y) ranges from 0.0057 t ha Mj-1 mm-1 to 0.45 t ha Mj-1 mm-1. The spatial distribution is detailed in the Y coefficient map (Fig. 4b). In the latter 41.81% of study area corresponds to the value Y=0.44 t ha Mj-1 mm-1 which is an Mediterranean red and brown soils regosols association, then 20.91 % displays brown or red sandy soils, hydromorphic sandy soils (granite) association with Y=0.35, then 13.95 % corresponds to a hydromorphic sandy soil with iron concretions with Y value =0.4.

The map (Φ) (Fig. 4c) shows soil sensitivity to erosion which is computed in the range between 0 and 1. For our study area, it ranges between 0.32 and 0.54, indicating soil sensitivity to erosion of between 20 % and 50 % of the area according to Gavrilovic's classification. Whereas, 31.14 % of the area represents the high class of the Φ factor. The coefficient (Ja) presents the percentage of slope in the study area based on the digital elevation model (DEM), where the maximum slope in the map (Ja) reaches 154.14 %. Only 4.29 % of the total surface area presents a slope > 40 % and the minimum values are less than 10 % covering 52.46 % of the total surface area of the study area. The steep slope favors downstream runoff and sediment transport (Fig. 4d). Setting the parameters Xa, Y, and Ja in equation (3) generates the coefficient (Z) map (Fig. 4e). The results of (Table 5) show that areas with low to moderate erosion potential are the most dominant, accounting for 70.23 % of the surface area, while areas affected by high erosion intensity cover 31.14 %.

The combination of data from the Gavrilovic factors (equation 1) presents the results of the erosion potential in study area (Fig. 6a and 7). The estimated erosion rate is between a minimum of 0,001 $m^3/km^2/y$ and a maximum of 68.26 $m^3/km^2/y$. However, an area of 758 km^2 hasn't insignificant erosion; then 25,73 % of the study area was subject to low erosion. Additionally, a surface area of 17,19 % is marked by moderate erosion. High erosion affescts 9,52 % of the surface area, while severe erosion affects only 116 km^2 of the study area which corresponds to 6,31 %. The spatial distribution of erosion shows remarkable effects from the upstream to the downstream (Fig. 6a). The intensity of downstream erosion on lithologies, gullies, and Wadis is remarkable. The action of climatic factor, steep topography and lithology lead to significant and irreversible soil degradation in the Korifla sub-watershed. Furthermore, it is important to note that the study area is far from having catastrophic hydric erosion, which is expressed by a low maximum soil loss value of 68.26 $m^3/km^2/y$. This inequitable distribution is due to the impact of the factors that generate the EPM model. Results are verified in the field, as well as correlated with satellite images and previous data (Ezzaouini *et al*., 2020; Mahe *et al*., 2012). Satellite image with strong erosion sites according to the EPM method, constitutes a guide that illustrates the spatial

location of areas vulnerable to hydric erosion, enabling the extraction of a roc curve. The ROC is used to validate the reliability of the results to compare the Area Under the Curve (AUC) value with that indicated on the expert scale (Fawcett, 2006), implementing 162 high erosion sites. The true positive rate indicates the erosion values that are indicated, in contrast with the negative values that are not detected. The use of the ROC curve ensures that the method has been able to concretize accurate and real values, where the analytical procedure were conducted within the ArcMap 10.5 using the ArcSDM tool. The most satisfactory values of AUC are close to 1. In the present case study, the reliability value of the EPM method according to the AUC computation is 0.76, then it is therefore classified as good (Fig. 8).

Fig. 4: EPM model parameters for Korifla sub-watershed, (a) Xa, (b) Y, (c) Φ, (d) Ja, and (e) Z

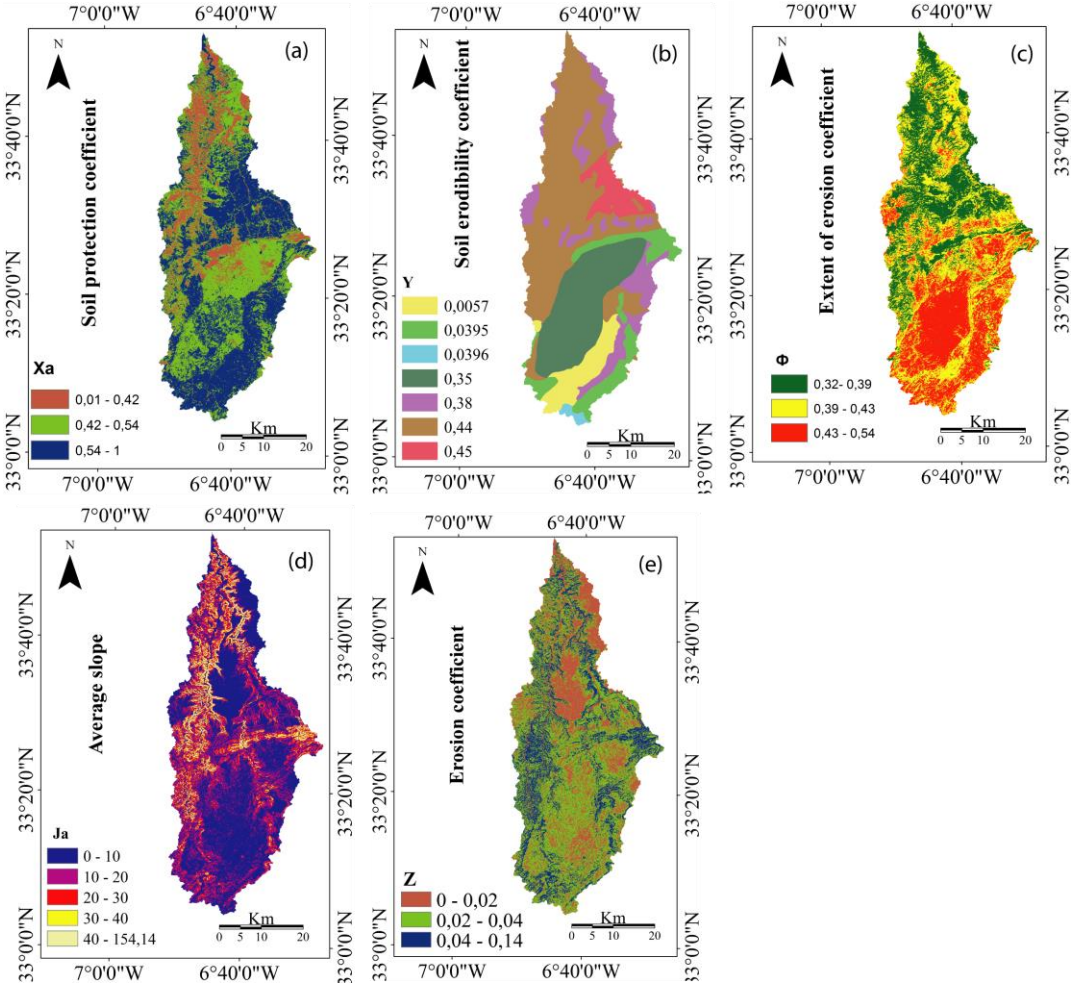

Fig. 5: Erodibility map and soil protection map According to PAP/RAC guidelines: (a) Erodibility map, and (b) Soil protection map

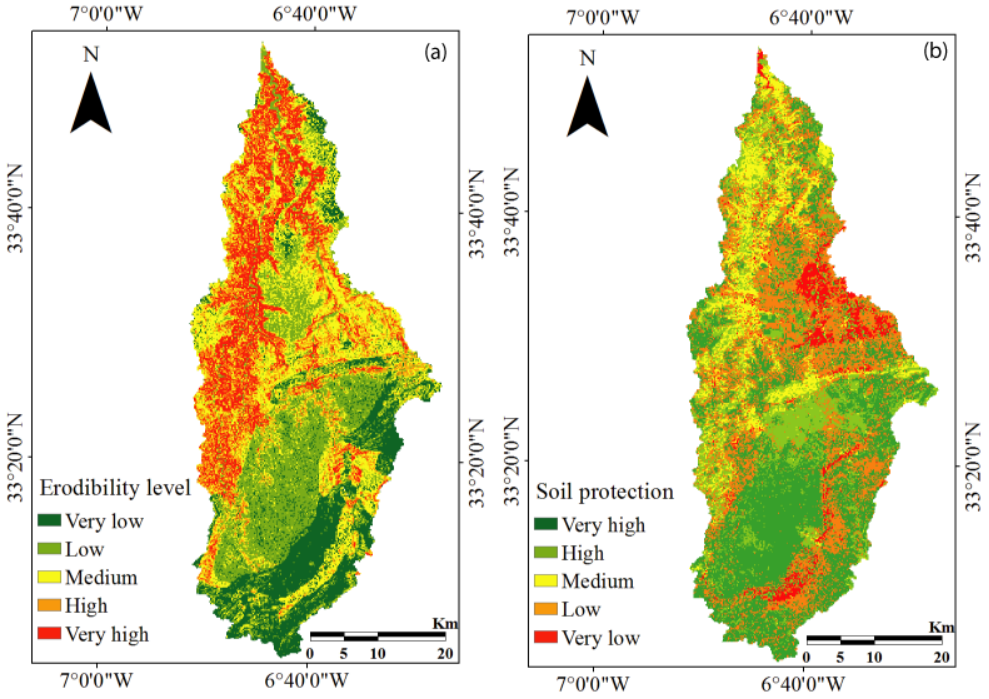

Fig. 6: Potential erosion maps, (a) EPM potential erosion estimation model, (b) PAP/RAC model

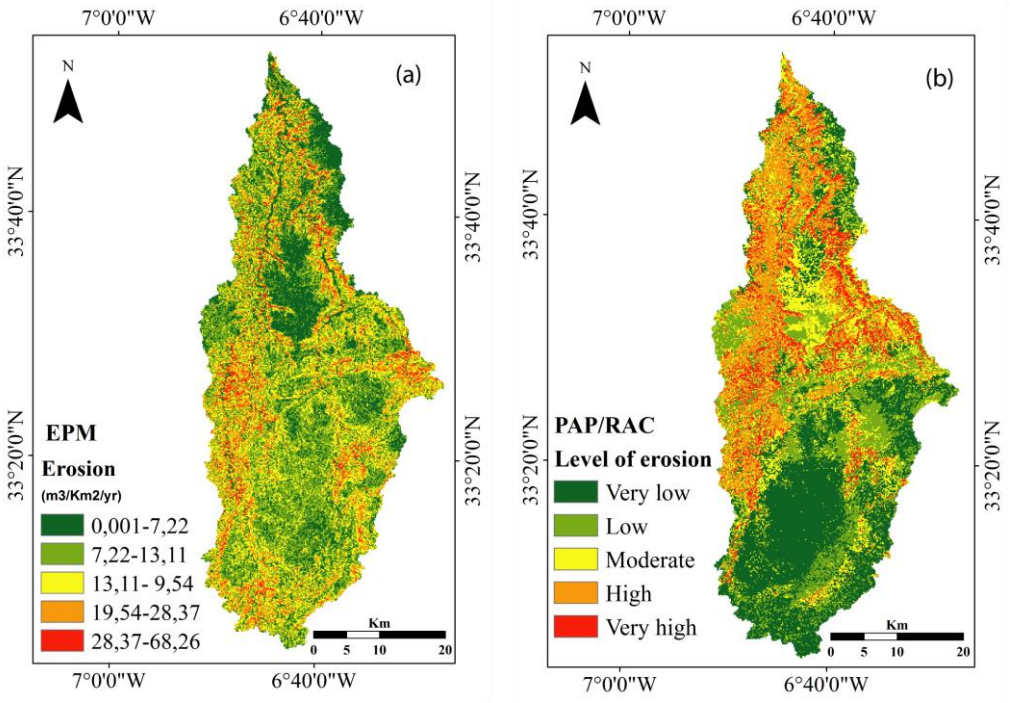

Fig. 7: Diagram of erosion intensity according to EPM and PAP/RAC models by area in $m^3/km^2/y$ (A) and in percentage (B)

Fig. 8: AUC ROC curve for EPM Model mapping results

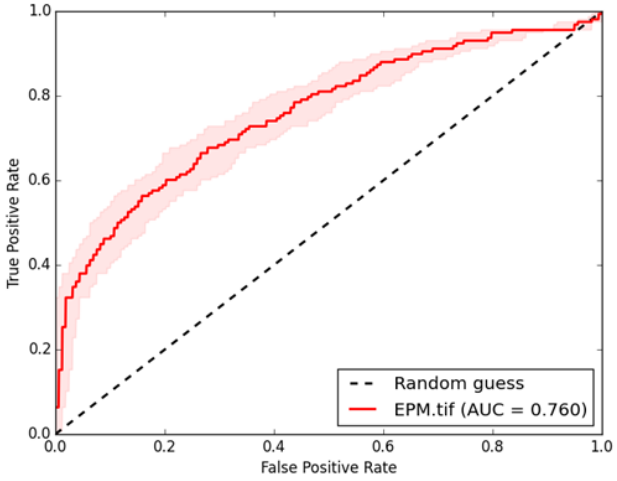

Table 5: Description of EPM parameters

Parameter	Value	Class	Area (%)
Extent of Erosion coefficient Φ	0,32-0,39	Low	30,22
	0,39-0,43	Moderate	38,64
	0,43-0,54	High	31,14
Erosion coefficient Z	0-0,02	High	29,77
	0,02-0,04	Moderate	47,31
	0,04-0,14	Low	22,92
	-	-	-
	-		-
Soil Erodibility coefficient Y	0,44	Red and brown soils	41,81
	0,35	Brown or red sandy soils, hydromorphic	20,91
	0,40	Hydromorphic sandy soils with iron concretions	13,95
	0,0395	Lithosols and regosols	9,64
	0,0057	Brown forest soils	7,16
	0,45	Red floors and turning	5,74
	0,44	Calcareous brown soils, steppe brown soils, lithosols	41,81
Soil protection coefficient Xa	0,01-0,42	High	15,47
	0,42-0,54	Moderate	40,35
	0,54-1	Low	44,17
Average Slope Ja	<10	Very low	52.46
	10%-20	Low	26 .55
	20%-30	Medium	11.35
	30%-40	High	5.35
	>40	Very high	4,29

PAP/RAC

The erosion assessment in the study area is based on two key maps using PAP/RAC model, the erodibility map and the soil protection map together form the base to define the erosive state. These maps are further supported by the consolidated PAP/RAC map.

The erodibility in the study area was categorized into five representative classes. The distribution of these classes is as follows: very low erodibility (covers 18.16 %), low erodibility (covers 24.28 %), medium erodibility (covers 28.24 %), high erodibility (covers 13.04 %), and very high erodibility covering 16.28 % of the total sub-watershed area. These

classes provide a comprehensive representation of the erosion susceptibility across the study area, allowing a detailed assessment of the erosive state and contributing to soil protection and erosion control strategies. Erodibility within the study area exhibits a close association with slope steepness zones Fig. 3d and 5a). The zones with steep to moderate slopes are experiencing a higher erosion susceptibility compared to the zones with gentle slopes. Moreover, vegetation plays a crucial role in mitigating runoff and erosion by promoting water infiltration (Cerdà *et al*., 2017). Additionally, vegetation factor enhances soil cohesion, thereby improving mechanical properties (O'Loughlin & Zhang, 1986).

The soil protection map is developed based on the degree of vegetation cover and land use patterns. The distribution of the soil protection classes is as follows: areas classified as having very high soil protection cover 35.41 % of the total area, high soil protection covers 19.55 %, medium soil protection covers 12.07 %, low soil protection covers 27.33 %, and very low soil protection covers 5.64 %. These values provide insights into the varying degrees of soil protection and vegetation cover across the study area. The map serves as a valuable tool for identifying areas with high and low soil protection, aiding in the formulation of appropriate land management and conservation strategies to mitigate erosion risks and protect soil resources. The lowest values are found in the zones where the vegetation index is less representative, hence the role of vegetation cover in protecting the soil against water erosion (Fig. 5b).

Furthermore, the interpretation of the consolidated PAP/RAC map results, presented in Figure 6b and 7, reveals that the rate of high erosion is relatively less concerning compared to other erosion values. The distribution of erosion categories across the study area is as follows: very high erosion covers 10.31 % of the area, high erosion covers 14.53 %, moderate erosion covers 20.07 %, low erosion covers 22.85 %, and very low erosion covers 32.24 %. It is important to note that field verification is required to validate the accuracy of the methodology and compare the actual results with those obtained through this approach. The integration of the Erosion Predictability Model (EPM) and the PAP/RAC maps demonstrates the cohesion between these two mapping methods, further enhancing the reliability of the erosion assessment.

EPM and PAP/RAC synergistic application and implications

The application of EPM and PAP/RAC yields distinct information. The two models are a valuable erosion assessment tools and can be effectively utilized with each other to obtain more complete comprehension of hydric erosion behavior. The present study results highlight the assessment and the mapping of erosion susceptibility in the Korifla sub-watershed using the EPM and PAP/RAC models. The extracted erosion potential map using EPM model the permitted successfully (AUC=76) the mapping of very high hydric erosion zones. These zones cover 6.31 % (116 $m^3/km^2/y$), followed by high erosion zones that cover 9.52 % (175 $m^3/km^2/y$) of the study area according to the EPM model. The analysis of EPM provides valuable insights into areas sensitivity to high-very high erosion which appear mainly in the low soil protection values (Xa), steep slope values (Ja), and high erosion coefficient values (Z) (Fig. 4a, d, and e). Besides, using PAP/RAC, the consolidated map by integrating erodibility map and soil protection layers allows the mapping of erodibility levels within Korifla sub-watershed. This map established on the basis on slope, lithology, vegetation and LULC allows the detection of the very high hydric erosion zones that represent 10.31 % of the area. High levels of erosion were observed downstream showing more sensitivity to moderate to high slopes in forest and agricultural lands. The hydric erosion mapping results reveal low hydric erosion in the study area, where, a good compatibility between EPM and PAP/RAC was observed. Accordingly, the previous works

of hydric erosion mapping in Bouregreg watershed rank the latter with low hydric erosion rates (Laouina & Mahé, 2013). Previous studies have focused mainly on the Bouregreg watershed and they were quantitative. (Hara *et al*., 2020) used RUSLE and USLE methods, and estimated the hydric erosion between 0 (t/ha/y) and 849 (t/ha/y). Hydric erosion is one of the most causes of soil loss. Taking into consideration Eddefli *et al*. (2023) study findings in Korifla sub-watershed, a good correlation between medium to high soil loss (maximum of 27.61 t/ha/y) zones and potential hydric erosion zones is noticed. As a limitation, the comparison of hydric erosion values between EPM (Fig. 6a) and PAP/RAC (Fig. 6b) cannot be faithful to reality. One gives a quantitative estimate of the rate of soil loss over the entire study area, while the other applies guidelines that classify areas according to the degree of erosion with a well-defined classification and spatial distribution without indicating soil loss values. However, hydric erosion in the study area varies spatially, with variations in the impact of the influencing factors of erosion extent. In global, the consolidated PAP/RAC map provides a comprehensive overview of erosion categories, with low to moderate erosion being the most dominant across the study area. Observation of the two final maps from the two methods shows cohesion between the results. As shown in figure 9 several field photographs along the Korifla Sub-watershed were token during field surveys. Following field observations, hydric erosion was controlled in the Korifla sub-watershed by the lithological diversity, the slope, and the plateaus and hills topography criteria. Hydric erosion is a process in which water progressively erodes through gullies or channels (Figure 9). Hydric erosion is accentuated in areas where the erosion rate (based on EPM) is high and the PAP /RAC class of erosion is very high. This suggests that this form of erosion (hydric erosion) is significant and predominant in the Korifla sub-watershed. Sandy and clay soils are the most vulnerable to erosion. Topography also contributes to hydric erosion, as run-off water from rainfall can collect in gullies and valleys, intensifying the erosion process. Other factors such as vegetation, soil cover and farming practices also influence the rate of erosion in the area. The implementation of soil conservation and water management measures can be considered to mitigate the effects of hydric erosion and preserve soil quality in the Korifla sub-watershed. The majority of the maximum soil loss values are perfectly aligned with the high erosion zones. The integration of the EPM and PAP/RAC mapping methods enhances the reliability of the erosion assessment. Overall, these results highlight the complex interplay of various factors influencing erosion susceptibility in the study area. The findings can serve as a basis for developing targeted erosion control and soil conservation strategies to mitigate erosion risks and protect valuable soil resources.

Fig. 9: Field photographs of hydric erosion of the Korifla sub-watershed, and their geographic location on the PAP/RAC-derived map.

The field observations show that sandy and clay soils are the most vulnerable to hydric erosion (b-j). Topography is demonstrated to have an important influence to hydric erosion (b, c, d and e). In addition, Land use and land cover influence directly the rate of soil erosion, where the vegetation cover is a mitigation factor of hydric erosion (f,g).

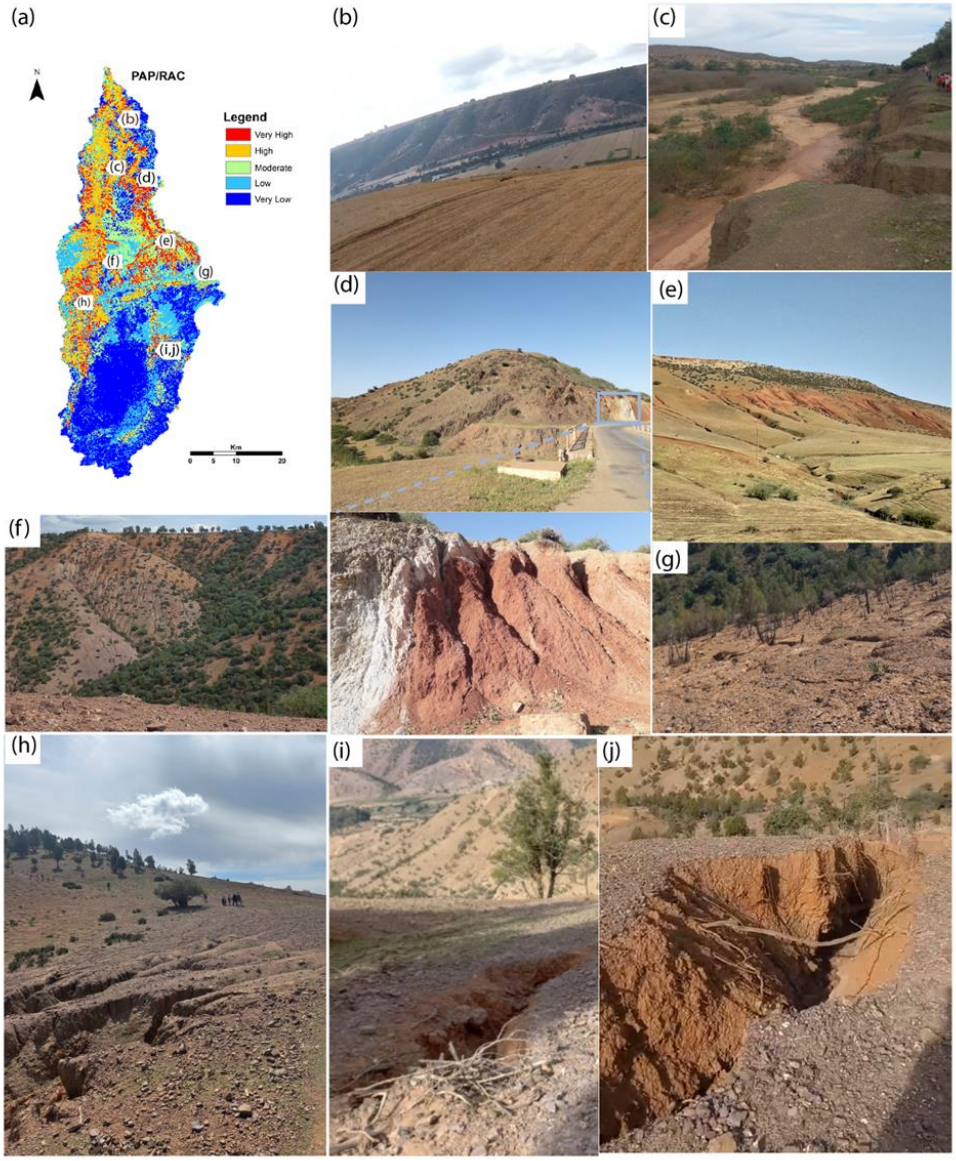

CONCLUSION

The study of soil loss in the Korifla watershed helps to estimate the sediment yield. EPM and PAP/RAC models were applied based on several natural parameters involved in hydric erosion. Furthermore, they were processed in a geographic information system environment and coupled with field observations to enhance erosion mapping in the study area. The EPM results show the soil loss in the Korifla sub-watershed varies between 0.001 ($m^3/km^2/year$) and 68.26 ($m^3/km^2/year$) which is far from catastrophic erosion risk, but could be considered as significant hydric erosion with moderate and high erosion potential. The PAP/RAC method has enabled us to accurately classify the most vulnerable areas to water erosion.

These results can be used, on the one hand, to implement the necessary soil conservation measures in vulnerable areas to water erosion in the basin. On the other hand, this study's findings can be beneficial to develop and manage areas not affected by water erosion. However, this study data suggest that a decision to address the causes and consequences of the hydric erosion trend should be made within the study area. To sum up, PAP/RAC guidelines can be supported by EPM to assess hydric erosion in semi-arid regions.

In light of the findings in this study, the application of synergistic approaches in hydric erosion assessment holds promising future possibilities. The use of EPM and PAP/RAC models in combination with geographic information systems and field observations has proven effective in providing a comprehensive understanding of erosion dynamics in the Korifla watershed. These integrated methods have not only facilitated the identification of vulnerable areas but also offered valuable insights for potential soil conservation measures and sustainable land management practices. Looking ahead, the incorporation of advanced technologies, remote sensing data, and machine learning techniques can further refine the accuracy and predictive capabilities of erosion models, as demonstrated for various environmental threats assessment in the worldwide (Jari *et al.*, 2023). Additionally, the dissemination of such research and its applicability to semi-arid regions underscores the importance of continued interdisciplinary efforts to address and mitigate the causes and consequences of hydric erosion, ultimately contributing to the preservation of critical ecosystems and the sustainable management of valuable natural resources.

ACKNOWLEDGMENT

The authors wish to thank Bouregeg and Chaouia Hydraulic Bassin Agency for providing rainfall data. They acknowledge the support from Sultan Moulay Slimane University. Acknowledgement to Journal of Landscape Ecology editor and the anonymous reviewer for their helpful remarks and recommendations to improve considerably the manuscript quality.

CONFLICT OF INTEREST

The authors declare no conflict of interest.

REFERENCES

Ahmed, A., Adil, D., Hasna, B., Elbachir, A., and Lazaar, R., (2019). Using EPM Model and GIS for estimation of soil erosion in Souss Basin, Morocco: *Turkish Journal of Agriculture-Food Science and Technology*, v. 7, no. 8, p. 1228-1232.

Alewell, C., Borrelli, P., Meusburger, K., and Panagos, P., (2019). Using the USLE: Chances, challenges and limitations of soil erosion modelling: *International soil and water conservation research*, v. 7, no. 3, p. 203-225.

Alitane, A., Essahlaoui, A., El Hafyani, M., El Hmaidi, A., El Ouali, A., Kassou, A., El Yousfi, Y., van Griensven, A., Chawanda, C. J., and Van Rompaey, A., (2022). Water erosion monitoring and prediction in response to the effects of climate change using RUSLE and SWAT equations: case of R'Dom watershed in Morocco: *Land*, v. 11, no. 1, p. 93.

Amini, H., Honarjoo, N., Jalaliyan, A., Khalilizadeh, M., and Baharlouie, J., (2014). A comparison of EPM and WEPP models for estimating soil erosion of Marmeh Watershed in the South Iran: *Poljoprivreda i Sumarstvo*, v. 60, no. 4, p. 299.

Badraoui, A., and Hajji, A., (2001). Envasement des retenues de barrages: La Houille Blanche, no. 6-7, p. 72-75.

Baharvand, S., and Pradhan, B., (2022). Erosion and flood susceptibility evaluation in a catchment of Kopet-Dagh mountains using EPM and RFM in GIS: *Environmental Earth Sciences*, v. 81, no. 20, p. 490.

Beaudet, G., (1969). *Le plateau central marocain et ses bordures: étude géomorphologique*: The Moroccan central plateau and its borders: geomorphological study. Rabbat. French and Moroccan Printing House pp. 478.

Biswakarma, P., Joshi, V., Abdo, H. G., Almohamad, H., Abdullah, A., and Al-Mutiry, M., (2023). An integrated quantitative and qualitative approach for landslide susceptibility mapping in West Sikkim district, Indian Himalaya: *Geomatics, Natural Hazards and Risk* v. 14.

Cerdà, A., Keesstra, S., Rodrigo-Comino, J., Novara, A., Pereira, P., Brevik, E., Giménez-Morera, A., Fernández-Raga, M., Pulido, M., and Di Prima, S., (2017). Runoff initiation, soil detachment and connectivity are enhanced as a consequence of vineyards plantations: *Journal of environmental management*, v. 202, p. 268-275.

Chikh, H. A., Habi, M., and Morsli, B., (2019). Influence of vegetation cover on the assessment of erosion and erosive potential in the Isser marly watershed in northwestern Algeria—comparative study of RUSLE and PAP/RAC methods: *Arabian Journal of Geosciences*, v. 12, p. 1-23.

De Roo, A., (1998). Modelling runoff and sediment transport in catchments using GIS: *Hydrological processes*, v. 12, no. 6, p. 905-922.

Diani, K., Ettazarini, S., Hahou, Y., El Belrhiti, H., Allaoui, W., Mounir, K., and Gourfi, A., (2023). *Identification of soil erosion sites in semiarid zones*: Using GIS, remote sensing, and PAP/RAC model, Handbook of Hydroinformatics, Elsevier, p. 169-183.

Eddefli, F., Ouakil, A., Khaddari, A., and Tayebi, M., (2023). Modeling Soil Erosion Using RUSLE and GIS--A Case Study of Korifla Sub-Watershed (Central Morocco): *Ecological Engineering & Environmental Technology* (EEET), v. 24, no. 4.

Efthimiou, N., and Lykoudi, E., (2016). Soil erosion estimation using the EPM model: *Bulletin of the Geological Society of Greece*, v. 50, no. 1, p. 305-314.

El Garouani, A., Merzouk, A., Jabrane, R., and Boussema, M., (2003). Cartographie de l'érosion des sols dans le bassin versant de l'Oued Jemâa (Pré-rif, Maroc): *Géomaghreb*, v. 1, no. 1, p. 39-46.

El Jazouli, A., Barakat, A., Khellouk, R., Rais, J., and El Baghdadi, M., (2019). Remote sensing and GIS techniques for prediction of land use land cover change effects on soil

erosion in the high basin of the Oum Er Rbia River (Morocco): *Remote Sensing Applications: Society and Environment*, v. 13, p. 361-374.

Elbadaoui, K., Mansour, S., Ikirri, M., Abdelrahman, K., Abu-Alam, T., and Abioui, M., (2023). Integrating Erosion Potential Model (EPM) and PAP/RAC Guidelines for Water Erosion Mapping and Detection of Vulnerable Areas in the Toudgha River Watershed of the Central High Atlas, Morocco: *Land*, v. 12, no. 4, p. 837.

Ezzaouini, M. A., Mahé, G., Kacimi, I., and Zerouali, A., (2020). Comparison of the MUSLE model and two years of solid transport measurement, in the Bouregreg Basin, and impact on the sedimentation in the Sidi Mohamed Ben Abdellah Reservoir, Morocco: *Water*, v. 12, no. 7, p. 1882.

Fawcett, T., (2006). An introduction to ROC analysis: *Pattern recognition letters*, v. 27, no. 8, p. 861-874.

Gavrilovic, Z., (1988). Use of an Empirical Method (Erosion Potential Method) for Calculating Sediment Production and Transportation in Unstudied or Torrential Streams, *in Proceedings International Conference on River Regime* (p 411-422), Hydraulics Research Limited, Wallingford, Oxon UK. 1988. p 411-422, 5 fig, 4 tab, 8 ref.1988.

Gocić, M., Dragićević, S., Radivojević, A., Martić Bursać, N., Stričević, L., and Đorđević, M., (2020). Changes in soil erosion intensity caused by land use and demographic changes in the Jablanica River Basin, Serbia: *Agriculture*, v. 10, no. 8, p. 345.

Hagras, A., (2023). Estimating water erosion in the EL-Mador Valley Basin, South-West Matrouh City, Egypt, using revised universal soil loss equation (RUSLE) model through GIS: *Environmental Earth Sciences*, v. 82, no. 1, p. 47.

Hara, F., Achab, M., Emran, A., and Mahe, G., (2020). Study of soil erosion risks using RUSLE Model and remote sensing: case of the Bouregreg watershed (Morocco): *Proceedings of the International Association of Hydrological Sciences* (p. 159-162), v. 383,.

Hili, A., Gartet, J., and EL Khalki, Y., (2017). Estimation qualitative de l'érosion hydrique dans le bassin versant de l'Oued Amlil par la combinaison de l'outil SIG et de l'approche PAP/CAR: *Espace Géographique et Société Marocaine*, no. 18.

Jari, A., Khaddari, A., Hajaj, S., Bachaoui, E. M., Mohammedi, S., Jellouli, A., Mosaid, H., El Harti, A., and Barakat, A., (2023). Landslide Susceptibility Mapping Using Multi-Criteria Decision-Making (MCDM), Statistical, and Machine Learning Models in the Aube Department, France: *Earth*, v. 4, no. 3, p. 698-713.

Kouhpeima, A., Hashemi, S. A. A., and Feiznia, S., (2011). A study on the efficiency of Erosion Potential Model (EPM) using reservoir sediments: *Elixir Pollution*, v. 38, p. 4135-4139.

Laouina, A., and Mahé, G., (2013). *Sustainable Land Management*. Proceedings of the multi-stakeholder meeting on the Bouregreg basin, 2013.

Mahe, G., Emran, A., Brou, Y. T., and Bi, Z. T., (2012). Analyse statistique de l'évolution de la couverture végétale à partir d'images Modis et Noaa sur le bassin versant du Bouregreg (Maroc): *Géo Observateur*, no. 20, p. 33--44.

Marouane, L., Lahcen, B., and Valérie, M., (2021). Assessment and mapping of water erosion by the integration of the Gavrilovic "EPM" model in the Inaouene watershed, Morocco, *in Proceedings E3S Web of Conferences 2021* (p. 03009), Volume 314, EDP Sciences.

Mesrar, H., Sadiki, A., Navas, A., Faleh, A., Quijano, L., and Chaaouan, J., (2015). Modélisation de l'érosion hydrique et des facteurs causaux, Cas de l'oued Sahla, Rif Central, Maroc: *Zeitschrift für geomorphologie*, v. 59, no. 4, p. 495-514.

Mosaid, H., Barakat, A., Bustillo, V., and Rais, J., (2022). Modeling and mapping of soil water erosion risks in the Srou Basin (Middle Atlas, Morocco) using the EPM model, GIS and magnetic susceptibility: *Journal of Landscape Ecology*, v. 15, no. 1, p. 126-147.

Moudden, F., El Hafyani, M., El Ouali, A., Roubil, A., El Ouali, A., Essahlaoui, A., and Brouziyne, Y., (2022). Diachronic mapping and evaluation of soil erosion rates using RUSLE in the Bouregreg River Watershed, Morocco: *Journal of Water and Land Development*, p. 86-99-86-99.

Nunes, A. N., De Almeida, A. C., and Coelho, C. O., (2011). Impacts of land use and cover type on runoff and soil erosion in a marginal area of Portugal: *Applied Geography*, v. 31, no. 2, p. 687-699.

O'Loughlin, C., and Zhang, X., (1986). The influence of fast-growing conifer plantations on shallow landsliding and earthflow movement in New Zealand steeplands, *in Proceedings 18th IUFRO World Congress*, Ljubljana (Yugoslavia), IUFRO1986.

Othman, A., El-Saoud, W. A., Habeebullah, T., Shaaban, F., and Abotalib, A. Z., (2023). Risk assessment of flash flood and soil erosion impacts on electrical infrastructures in overcrowded mountainous urban areas under climate change: *Reliability Engineering & System Safety*, v. 236, p. 109302.

PAP/CAR, (1998). *Directives pour la cartographie et la mesure des processus d'erosion hydrique dans les zones cotieres mediterraneennes.* PAP-8/PP/GL.1 Split, Centre d'activités régionales pour le Programme d'Actions prioritaires, 72 p

Pavlova-Traykova, E., (2022). using the epm method for the estimation of soil erosion in forest territories in the upper part of Dzherman River: *Silva Balcanica*, v. 23, no. 2, p. 19-25.

Rhouma, A. B., Hermassi, T., and Bouajila, K., (2018). Water erosion modeling using the pap/car qualitative method: case of the sbaihia catchment, Zaghouan: *Journal of New Sciences*, v. 51, p. 3225-3236.

Ristić, R., Radić, B., Vasiljević, N., and Nikić, Z., (2011). Land use change for flood protection: A prospective study for the restoration of the river Jelašnica watershed: *Glasnik Sumarskog fakulteta*, no. 103, p. 115-130.

Siddique, M., Sultana, J., Abdullah, M., and Azad, K., (2017). Modelling of soil loss through RUSLE2 for soil management in an agricultural field of Uccle, Belgium: *British Journal of Environment and Climate Change*, v. 7, no. 4, p. 252-260.

Staut, M., (2004). *Recent erosional processes in the catchment of the Dragonja river*: Unpublished graduate thesis. Faculty of Arts, University of Ljubljana, Ljubljana.(In Serbian).

Tangestani, M. H., (2006). Comparison of EPM and PSIAC models in GIS for erosion and sediment yield assessment in a semi-arid environment: Afzar Catchment, Fars Province, Iran: *Journal of Asian earth sciences*, v. 27, no. 5, p. 585-597.

Tucker, C. J., (1979). Red and photographic infrared linear combinations for monitoring vegetation: *Remote sensing of Environment*, v. 8, no. 2, p. 127-150.

Zahnoun, A. A., Makhchane, M., Chakir, M., Al Karkouri, J., and Watfae, A., (2019). Estimation and cartography the water erosion by integration of the Gavrilovic "EPM" model using a GIS in the Mediterranean watershed: Lower Oued Kert watershed (Eastern Rif,

Morocco): *International Journal of Advance Research, Ideas and Innovations in Technology*, v. 5, p. 367-374.

Zorn, M., and Komac, B., (2009). Response of soil erosion to land use change with particular reference to the last 200 years (Julian Alps, Western Slovenia): *Revista de geomorfologie*, v. 11, p. 39-47.